Dynamic Contrast-enhanced Area-detector CT vs Dynamic Contrast-enhanced Perfusion MRI vs FDG-PET/CT: Comparison of Utility for Quantitative Therapeutic Outcome Prediction for NSCLC…

Seki, Shinichiro ; Fujisawa, Yasuko ; Yui, Masao ; Kishida, Yuji ; Koyama, Hisanobu ; Ohyu, Shigeharu ; Sugihara, Naoki ; Yoshikawa,…

(Citation)
Magnetic Resonance in Medical Sciences,19(1):29-39

(Issue Date)
2020

(Resource Type)
journal article

(Version)
Version of Record

Magn Reson Med Sci 2020; 19; 29–39
doi:10.2463/mrms.mp.2018-0158
Published Online: March 18, 2019

MAJOR PAPER

Dynamic Contrast-enhanced Area-detector CT vs Dynamic Contrast-enhanced Perfusion MRI vs FDG-PET/CT: Comparison of Utility for Quantitative Therapeutic Outcome Prediction for NSCLC Patients Undergoing Chemoradiotherapy

Shinichiro Seki[1,2], Yasuko Fujisawa[3], Masao Yui[3], Yuji Kishida[4], Hisanobu Koyama[4], Shigeharu Ohyu[3], Naoki Sugihara[3], Takeshi Yoshikawa[1,2], and Yoshiharu Ohno[1,2*]

Purpose: To directly compare the utility for therapeutic outcome prediction of dynamic first-pass contrast-enhanced (CE)-perfusion area-detector computed tomography (ADCT), MR imaging assessed with the same mathematical method and 2-[fluorine-18]-fluoro-2-deoxy-D-glucose–positron emission tomography combined with CT (PET/CT) for non-small cell lung cancer (NSCLC) patients treated with chemoradiotherapy.

Materials and Methods: Forty-three consecutive stage IIIB NSCLC patients, consisting of 25 males (mean age ± standard deviation: 66.6 ± 8.7 years) and 18 females (66.4 ± 8.2 years) underwent PET/CT, dynamic CE-perfusion ADCT and MR imaging, chemoradiotherapy, and follow-up examination. In each patient, total, pulmonary arterial, and systemic arterial perfusions were calculated from both perfusion data and SUV_{max} on PET/CT, assessed for each targeted lesion, and averaged to determine final values. Receiver operating characteristics analyses were performed to compare the utility for distinguishing responders from non-responders using Response Evaluation Criteria in Solid Tumor (RECIST) 1.1 criteria. Overall survival (OS) assessed with each index were compared between two groups by means of the Kaplan–Meier method followed by the log-rank test.

Results: Area under the curve (Az) for total perfusion on ADCT was significantly larger than that of pulmonary arterial perfusion ($P < 0.05$). Az of total perfusion on MR imaging was significantly larger than that of pulmonary arterial perfusion ($P < 0.05$). Mean OS of responder and non-responder groups were significantly different for total and systemic arterial ($P < 0.05$) perfusion.

Conclusion: Dynamic first-pass CE-perfusion ADCT and MR imaging as well as PET/CT are useful for early prediction of treatment response by NSCLC patients treated with chemoradiotherapy.

Keywords: *computed tomography, magnetic resonance imaging, non-small cell lung cancer, positron emission tomography combined with computed tomography, therapeutic effect*

Introduction

Based on the evidence of a meta-analysis showing the superiority of concurrent chemotherapy and thoracic radiation therapy (i.e. chemoradiotherapy) to sequential chemoradiotherapy for unresectable stage III non-small cell lung cancer (NSCLC), with a 2- and 5-year absolute survival benefits of 10% and 4.5%, respectively,[1] radiation oncologists must evaluate whether the patients are suitable for chemoradiotherapy. Until now, the eligibility criteria for chemoradiotherapy were not precisely defined. In addition, early prediction of therapeutic effect may make it possible for physicians including

[1]Division of Functional and Diagnostic Imaging Research, Department of Radiology, Kobe University Graduate School of Medicine, 7-5-2 Kusunoki-cho, Chuo-ku, Kobe, Hyogo 650-0017, Japan

Received: November 29, 2018 | Accepted: February 6, 2019

[2]Advanced Biomedical Imaging Research Center, Kobe University Graduate School of Medicine, Hyogo, Japan
[3]Canon Medical Systems Corporation, Tochigi, Japan
[4]Division of Radiology, Department of Radiology, Kobe University Graduate School of Medicine, Hyogo, Japan
*Corresponding author, Phone: +81-78-382-6104, Fax: +81-78-382-6129, E-mail: yosirad@kobe-u.ac.jp; yosirad@med.kobe-u.ac.jp; yoshiharuohno@aol.com

radiation oncologists, oncologist, pulmonologist and patients to consider treatment options for personalized medicine, and thus has the potential to improve quality of life for NSCLC patients both during and after treatment.

For this clinical issue, two dynamic imaging techniques, dynamic contrast-enhanced (CE) perfusion CT and dynamic CE-MR imaging, diffusion-weighted MR imaging and positron emission tomography (PET) or PET combined with CT (PET/CT) using 2-[fluorine-18]-fluoro-2-deoxy-D-glucose (FDG) has been suggested as useful for evaluating tumor perfusion parameters as well as glucose metabolism, etc.[2–15] Moreover, dynamic CE-perfusion CT using a 320-detector row CT scanner with an area detector CT (ADCT) has been recommended as a useful tool for quantitative perfusion evaluation for lung nodule, therapeutic effect prediction in NSCLC patients.[16–18] In addition, a mathematical model was found to be an important factor for quantitative perfusion parameter evaluation in this setting. On the other hand, quantitatively assessed dynamic CE-perfusion MR imaging has been introduced as useful for evaluation of diagnosis of therapeutic effect as well as assessment of disease severity of pulmonary vascular diseases.[19–24] Under these circumstances, there seems to be an urgent need for reproducible assessment of quantitative pulmonary perfusion parameters on dynamic CE-perfusion CT and MR imaging using the same mathematical models at 3T MR system. To the best of our knowledge, however, no studies have been reported of a direct comparison of dynamic CE-perfusion ADCT and MR imaging, which are analyzed using the same mathematical model, with PET/CT for therapeutic effect prediction for NSCLC patients treated with chemoradiotherapy.

We hypothesized that quantitatively assessed dynamic CE-perfusion ADCT and MR imaging using the same mathematical model have potential for therapeutic effect prediction similar to that of PET/CT for NSCLC patients treated with chemoradiotherapy. The purpose of this study was therefore to directly compare the utility for therapeutic outcome prediction of dynamic CE-perfusion ADCT and MR imaging assessed with the same mathematical method and FDG-PET/CT for NSCLC patients treated with chemoradiotherapy.

Materials and Methods

Subjects

This prospective study was approved by the Institutional Review Board of Kobe University Hospital and written informed consent was obtained from all patients.

From January to December 2016, a total of 53 patients, consecutively and pathologically diagnosed with NSCLC and clinically diagnosed as stage IIIB, comprised of 29 men (mean age ± standard deviation: 68.1 ± 11.3 years) and 24 women patients (67.1 ± 9.4 years) and underwent dynamic CE-perfusion ADCT, dynamic CE-perfusion MR imaging and FDG-PET/CT. All radiological examinations were performed in random order within 2 weeks (mean: 6 days; range: 1–14 days). The diagnosis was based on the results of contrast-enhanced whole-body CT, FDG-PET/CT, contrast-enhanced brain MRI, body MR imaging including diffusion-weighted imaging, bone scintigraphy and pathological examination of specimens obtained by transbronchial and/or CT-guided biopsies according to the criteria for staging by the International Union Against Cancer. All studies were performed in random order within 3 weeks of diagnosis and before treatment. The patients included in this study were selected according to the following criteria: a) tumor measuring 10 mm in diameter or more; b) no prior history of chemotherapy or thoracic radiotherapy; c) Eastern Cooperative Oncology Group performance status ≤1; d) age ≤ 75 years; e) leukocytes ≥ 4000/μL, platelets ≥ 100000/μL, hemoglobin ≥ 9.5 g/dL, serum creatinine ≤ normal institutional upper limit, 24-h creatinine clearance ≥ 60 ml/min, bilirubin ≤ 1.5 mg/dL, aspartate aminotransferase (AST) and alanine aminotransferase (ALT) ≤ 2.0 × normal upper limit, and partial pressure of arterial oxygen ≥ 70 mmHg. Patients were excluded if they had 1) pulmonary fibrosis, 2) other active, invasive malignancies during the 3 years leading up to protocol entry, 3) malignant effusion, 4) pyrexia of 38°C or more at baseline, 5) infections, 6) significant cardiac disease, 7) uncontrolled diabetes mellitus, 8) paresis of the intestine ileus, or 9) regular use of corticosteroids.

Ten patients did not meet the inclusion criteria, so that the eventual study group comprised 43 consecutive patients, 25 males (mean age ± SD: 66.6 ± 8.7 years) and 18 females (66.4 ± 8.2 years). Pathological examination results identified 35 patients with adenocarcinoma, seven with squamous cell carcinoma, and one with large cell carcinoma. All patients were treated with chemoradiotherapy consisting of concurrent administration of thoracic radiotherapy and chemotherapy.

Therapeutic regimen for chemoradiotherapy

During thoracic radiotherapy (TRT) administration, all patients underwent concurrent chemotherapy. The latter consisted of vindesine (3 mg/m^2) on days 1 and 8, cisplatin (80 mg/m^2) on day 1, and mitomycin (8 mg/m^2) on day 1. The chemotherapy was repeated every 4 weeks for a total of four courses. On day 2 of chemotherapy, TRT was begun at a dose of 2 Gy/fraction administered in 15 fractions over 3 weeks, followed by a rest period of 1 week. Radiation was resumed at a dose of 2 Gy/fraction administered in 15 fractions over 3 weeks. The total dose of radiation administered was 60 Gy.

Evaluation of chemoradiotherapy response

Chest radiography, complete blood count, and blood chemistry studies were performed for all patients once a week during the treatment. The response in all targeted and non-targeted lesions was evaluated in accordance with the Response Evaluation Criteria in Solid Tumors (RECIST 1.1)[12,25] and by consensus of radiologists,

radiation oncologists, pulmonologists and oncologists who did not perform any of the image and/or statistical analyses for this study and had more than 10 years' experience in their respective specialties. After the treatment, chest radiographs or chest contrast-enhanced CTs were obtained every 3 months, and whole-body contrast-enhanced CT, brain contrast-enhanced MR imaging, bone scintigraphy and/or FDG-PET/CT every 6 months.

All patients were then divided into two groups, RECIST responders, consisting of the complete response (CR) and partial response (PR) groups, and RECIST non-responders, consisting of the stable disease (SD) and progressive disease (PD) groups. Overall survival (OS) and progression free survival (PFS) were evaluated for each group, with OS defined as the time from diagnosis until death from any cause, and PFS as the time between assignment for treatment and disease progression, death, or last known follow-up. The follow-up after finishing chemoradiotherapy ranged from 3 to 36 months.

Dynamic first-pass CE-perfusion ADCT examination

All dynamic first-pass CE-ADCT studies were performed on a 320-detector row CT scanner (Aquilion ONE; Canon Medical Systems, Tochigi, Japan) by means of a volumetric cine scan without helical scan.[14–18] All dynamic first-pass CE-perfusion ADCT were performed with volumetric scanning at two or three different positions to cover the entire lung. Dynamic ADCT examination was performed at an interval of at least 5 min between each volume position. The estimated volume computed tomography dose index ($CTDI_{vol}$ [e.g., pitch]) displayed on the CT scanner console was recorded for each patient. These values were based on the weighted CTDI ($CTDI_{w}$ [e.g., tube voltage or tube current]). $CTDI_{vol}$ obtained with each of the dynamic first-pass perfusion ADCT studies was 16.0 mGy. The estimated dose length product was calculated as $CTDI_{vol}$ × scan length, which was determined as 343.3–514.9 mGy × cm, with the effective dose for this protocol estimated at 4.81–7.21 mSv. The details of dynamic first-pass CE-perfusion ADCT examination are described in the literature.[14–18]

Dynamic first-pass CE-MR imaging with ultra-short TE using a 3T MR system

All MR studies were performed with a 3T superconducting magnet (Vantage Titan 3T; Canon Medical Systems) using a phased array coil (SPEEDER coil; Canon Medical Systems) with parallel imaging capability. In each subject, dynamic MR images (TR, 3.0 ms/TE, 1.1 ms/flip angle, 12°; reduction factor, 2; matrix, 256 × 64; reconstructed matrix, 512 × 128; FOV, 500 × 350 mm) were acquired with a 3D fast field echo sequence without fat suppression pulse. A 3D-slab with a thickness of 135 mm including the targeted lesions was used with 36 partitions in the coronal plane in a left-to-right phase-encoded direction, resulting in an effective partition thickness of 3.75 mm and real-phase encoding in the slice direction of 14 steps with partial Fourier reconstruction. This means that the spatial resolution of dynamic first-pass CE-MRI was 7.81 (*x*-axis) × 1.36 (*y*-axis) × 7.5 mm (*z*-axis), and the temporal resolution was 1.565 s (3 ms × 64 steps × 14 steps × 1/2 <reduction factor> with 21 ms fat suppression pre-pulse and 200 ms waiting time) for each 3D data set. About 1.0 ml of gadolinium contrast medium (Magnescope, Gadoterate meglumine [Gd-DOTA]; Guerbet Japan, Tokyo, Japan) was bolus administered to all patients through a cubital vein with an automatic infusion system (Sonic shot, Nemoto & Co., Ltd., Tokyo, Japan) at a rate of 5 ml/s, followed by 20 ml of saline solution at the same rate. The dynamic first-pass CE-MR sequence was initiated at the time of the contrast medium injection. The basic theory and application of dynamic first-pass CE-MR imaging have been documented in previous publications.[19–23] With each scan, 20 images were obtained during 32 s of breath holding at end-inspiration, and all 53 dynamic first-pass CE-MR examinations were completed successfully without any adverse effects.

Integrated FDG-PET/CT examinations

On FDG-PET/CT examination, each patient fasted for at least 6 h before the intravenous administration of FDG at a rate of 3.3 MBq/kg body weight (BW), and images were obtained from the skull to the mid-thigh 60 min after completion of the injection. All FDG-PET/CT examinations were performed with a commercially available PET/CT scanner (Discovery ST; GE Health Care, Milwaukee, WI, USA) and a standard lung cancer staging protocol stated in the past literatures.[14–18]

Image analysis

Image analysis of dynamic first-pass CE-perfusion ADCT and dynamic first-pass CE-perfusion MR imaging with ultra-short TE

All dynamic first-pass CE-perfusion ADCT and dynamic first-pass CE-perfusion MR imaging data were transferred to a personal computer (Precision; DELL, Kanagawa, Japan), and automated 3D motion corrections were performed with software, the details of which were published in a number of technical papers.[14–18] In addition, dynamic ADCT data obtained at each position were combined to generate dynamic first-pass CE-whole-lung perfusion ADCT images by means of commercially available software provided by Canon Medical Systems. Next, ROIs (diameter range: 6–79 mm) were placed by a chest radiologist with 22 years' experience (Y.O) over each targeted lesion, the main trunk of the pulmonary artery, the lung parenchyma and/or descending aorta. In addition, our proprietary CT software (Advanced Body Perfusion; Canon Medical Systems) and proprietary MR software (Canon Medical Systems), which was still in the developmental stage and not commercially available at the time, was used for all analyses. All quantitatively analyzed ADCT and MR indices were

analyzed on a pixel-by-pixel basis. An ROI was placed over each targeted lesion, encompassing its entire cross-sectional area, and made as large as possible to minimize the effects of tumoral hemodynamic inhomogeneities. For perfusion parameter measurements, ROIs were placed over all slices of a targeted lesion, and the indices determined for each slice were also averaged. All targeted lesions of a given patient were identified on the basis of RECIST criteria.[12,25] Density-time or signal intensity-time curves for all the tumors were generated for a mediastinal window setting or un-enhanced fast field echo (FFE) image that ensured that the need for partial volume averaging was minimized.

For this study, quantitatively analyzed ADCT and MR indices were calculated using the dual-input maximum slope method, selected on the basis of past study results.[14–18] To correct differences in transit time due to pulmonary and cardiac factors and calculate perfusion parameters by means of dual- and single-input maximum slope methods, ROIs were also placed over pulmonary artery and lung parenchyma in the opposite lung and aorta. All time-density course curves were then visually assessed for the calculation of each of the perfusion parameters while minimizing the above-mentioned effects of the software.

For the dual-input maximum slope model, a modification of the theories presented in previous publications[14–18] was used, which involved the calculation of total, pulmonary arterial and systemic arterial perfusions within a lesion with the following formulas [1] and [2]:

$$\text{Pulmonary arterial perfusion} = \frac{\text{Pulmonary arterial blood flow}}{\text{Volume of nodule}} = \frac{\mathrm{d}[C_{\mathrm{n}}(t)]/\mathrm{d}t_{\max}}{C_{\mathrm{a}}(t_{\max})} \quad [1]$$

$$\text{Systemic arterial perfusion} = \frac{\text{Descending aortic blood flow}}{\text{Volume of nodule}} = \frac{\mathrm{d}[C_{\mathrm{n}}(t)]/\mathrm{d}t_{\max}}{C_{\mathrm{s}}(t_{\max})} \quad [2]$$

where C_{n} is the concentration of contrast media within the tumor, C_{a} their concentration within the main trunk of the pulmonary artery, C_{s} their concentration within the descending aorta, t the time after contrast media injection, and $t_{\max}$ the time at maximal C_{a} or C_{s}.

Previous studies[14–18] have reported that lung tumors are supplied by both bronchial and pulmonary circulation, but metastatic lymph node sites are supplied predominantly by bronchial circulation. We therefore determined the total perfusion with the following formula [3]:

$$\text{Total perfusion} = \text{Pulmonary arterial perfusion} + \text{Systemic arterial perfusion} \quad [3]$$

For the dual-input maximum slope method,[15–18] total perfusion, pulmonary arterial perfusion and systemic arterial perfusion were calculated on the basis of systemic circulation within each lesion and expressed in ml/100 m/min.

To determine the utility for early prediction of therapeutic effect using dynamic CE-perfusion ADCT and MR indices, perfusion parameters within all targeted lesions were averaged to obtain the respective perfusion index-based biomarkers for the patients. Finally, each dynamic CE-perfusion index was measured twice for all patients, and the final value was determined as the average of the first and second measurements.

Image analysis of integrated FDG-PET/CT

For FDG-PET/CT images, standardized uptake value (SUV) data were overlaid on a conventional plain multiple detector CT with the lung window set for an FDG-PET/CT section thickness of 5 mm. ROIs (diameter range: 10–85 mm) were then placed by a general radiologist (T.Y) with 21 years' overall experience and more than 10 years' experience as a PET physician over all targeted lesions in each of the slices with reference to RECIST criteria[12,25] for determination of the maximum value of SUV (SUV_{max}). To minimize the effects of metabolic inhomogeneities within a targeted lesion, the ROI was made as large as possible and placed over the lesion so as to encompass its entire cross-sectional area. The SUV_{max} values for the slices were then averaged to obtain the mean SUV_{max} value at each of the measurement time points. SUV_{max} was measured twice and averaged to obtain the final value for a lesion as determined by each investigator.

Statistical analysis

For intra-observer agreement evaluation, the Bland–Altman analysis was used to compare the reproducibility coefficients of all dynamic first-pass CE-perfusion ADCT and MR indices,[26,27] while correlations between first and second measurements of each index were assessed by means of Pearson's correlation.

The relationship between dynamic first-pass CE-perfusion ADCT and MR imaging for each perfusion index was determined by means of Pearson's correlation. In addition, intra-method agreement for the perfusion index was assessed by means of Bland–Altman analysis.

For evaluation of differences between RECIST responders and non-responders for each dynamic CE-perfusion ADCT and MR index and SUV_{max} as well as for gender, age, performance status (PS), histological subtypes and tumor markers, all indices for the two groups were compared by means of χ^2 test, Wilcoxon's signed-rank test or Student's t-test. In addition, mean PFS and OS of the responder group were also statistically compared with those of the non-responder group using the Kaplan–Meier method followed by the log-rank test.

To determine the utility of each perfusion index and SUV_{max} as a marker for differentiation between RECIST responders and non-responders, receiver operating characteristics (ROC) were analyzed to determine feasible thresholds for all perfusion indices used to identify significant differences between the two groups. This was followed by a comparison of sensitivity, specificity and accuracy of the perfusion indices by means of McNemar's test.

To evaluate the capability of each index to have a significant influence on step-wise regression analysis for therapeutic effect prediction, PFSs and OSs for responder and non-responder groups in relation to each of the indices were compared using the Kaplan–Meier method followed by the log-rank test. In addition, a Cox proposal hazard regression model was applied as multivariate analyses for determination of predictors of PFS and OS including age, sex, patient's performance status, tumor marker and each index to have a significant influence on step-wise regression analysis for therapeutic effect prediction.

A *P*-value <0.05 was considered significant for all statistical analyses.

Results

Representative cases are shown in Fig. 1. These cases showed no adverse effects from the procedures used for this study. In addition, there were no patients who were excluded from image analysis due to poor image quality or the impossibility of body registration. Therapeutic effect evaluation was categorized into 23 cases as PR, 15 as SD and 5 as PD. The RECIST responder group consisted of 23 cases and the RECIST non-responder group of 20 cases.

Intra-observer agreement assessments

Correlation between the first and second measurements of each index on dynamic first-pass CE-perfusion ADCT, dynamic first-pass CE-perfusion MR imaging and PET/CT was significant and excellent ($r = 0.99$, $P < 0.0001$). On dynamic first-pass CE-perfusion ADCT, mean difference and reproducibility of all indexes between first and second measurements were as follows: total perfusion, 0 and 2.8 ml/100 ml/min; pulmonary arterial perfusion, 0 and 2.6 ml/100 ml/min; and systemic arterial perfusion, 0 and 2.4 ml/100 ml/min. On dynamic first-pass CE-perfusion MR imaging, mean difference and reproducibility coefficients for all indices between first and second measurements were as follows: total perfusion, 0 and 3.4 ml/100 ml/min; pulmonary arterial perfusion, 0 and 3.0 ml/100 ml/min; and systemic arterial perfusion, 0 and 3.1 ml/100 ml/min. Moreover, the mean difference in SUV_{max} between first and second measurements was 0, while the reproducibility coefficient for SUV_{max} was 0.1. The reproducibility coefficient for each index was <10% and thus satisfactory for clinical purposes.

Inter-method agreement assessment

Correlation for each index between the two methods were significant and excellent for dynamic first-pass CE-perfusion ADCT ($r = 0.99$, $P < 0.0001$) and for dynamic first-pass CE-perfusion MR imaging ($r = 0.99$, $P < 0.0001$). The limits of agreement between the two methods were determined as follows: total perfusion, -6.4 ± 1.1 ml/100 ml/min; pulmonary arterial perfusion, -0.93 ± 0.2 ml/100 ml/min; and systemic arterial perfusion, -6.0 ± 1.1 ml/100 ml/min. The limits of agreement for each perfusion index between the two methods were small enough for clinical purposes.

Comparisons of dynamic CE-perfusion ADCT indices as well as other clinical and patient parameters for RECIST responders and non-responders groups

Comparisons of gender, age, performance status, histological subtype, tumor marker, dynamic first-pass CE-perfusion ADCT indices, PFS and OS for the RECIST responder and RECIST non-responder groups are shown in Table 1. As for dynamic first-pass CE-perfusion ADCT indices, there were significant differences between the two groups for all perfusion parameters ($P < 0.05$). There were also significant differences for all perfusion parameters in terms of dynamic first-pass CE-perfusion MR indices ($P < 0.05$), SUV_{max} ($P = 0.002$), PFS ($P = 0.04$), and OS ($P = 0.006$).

Utility of radiological indices for differentiation of RECIST responders from RECIST non-responders

The results of ROC analysis of radiological indices, which disclosed significant differences between the RECIST responder and non-responder groups, are shown in Fig. 2. Area under the curve (Az) for each index on dynamic first-pass CE-perfusion ADCT was as follows: total perfusion, Az = 0.87 (95% confidence interval [CI]: 0.73–0.95); pulmonary arterial perfusion, Az = 0.72 (95% CI: 0.54–0.84); and systemic arterial perfusion, Az = 0.84 (95% CI:0.69–0.93). Moreover, Az for each index on dynamic first-pass CE-perfusion MR imaging was as follows: total perfusion, Az = 0.90 (95% CI: 0.77–0.96); pulmonary arterial perfusion, Az = 0.72 (95% CI: 0.54–0.84); and systemic arterial perfusion, Az = 0.84 (95% CI: 0.69–0.93). In addition, Az for SUV_{max} was assessed as 0.78 (95% CI: 0.60–0.90). Az for total perfusion on dynamic first-pass CE-perfusion ADCT was significantly larger than that for pulmonary arterial perfusion with both methods (ADCT: $P = 0.003$, MR imaging: $P = 0.003$). Moreover, Az for total perfusion on dynamic first-pass CE-perfusion MR imaging was significantly larger than that of pulmonary arterial perfusion with both methods (ADCT: $P = 0.002$, MR imaging: $P = 0.002$). The feasible threshold values for all indices on dynamic CE-perfusion ADCT were as follows: total perfusion, 29.2 ml/100 ml/min; pulmonary arterial perfusion, 15.5 ml/100 ml/min; and systemic arterial perfusion 11.0 ml/100 ml/min. Further, the feasible threshold values for all indices on dynamic CE-perfusion MR imaging were as follows: total perfusion, 37.5 ml/100 ml/min; pulmonary arterial perfusion, 16.3 ml/100 ml/min; and systemic arterial perfusion, 16.5 ml/100 ml/min, while the feasible threshold value for SUV_{max} was determined as 5.7.

Utility of all dynamic CE-perfusion ADCT and MR indices and SUV_{max} for differentiating the two groups is shown in Table 2. In addition, there were no significant differences among the indices in sensitivity, specificity, and accuracy ($P > 0.05$).

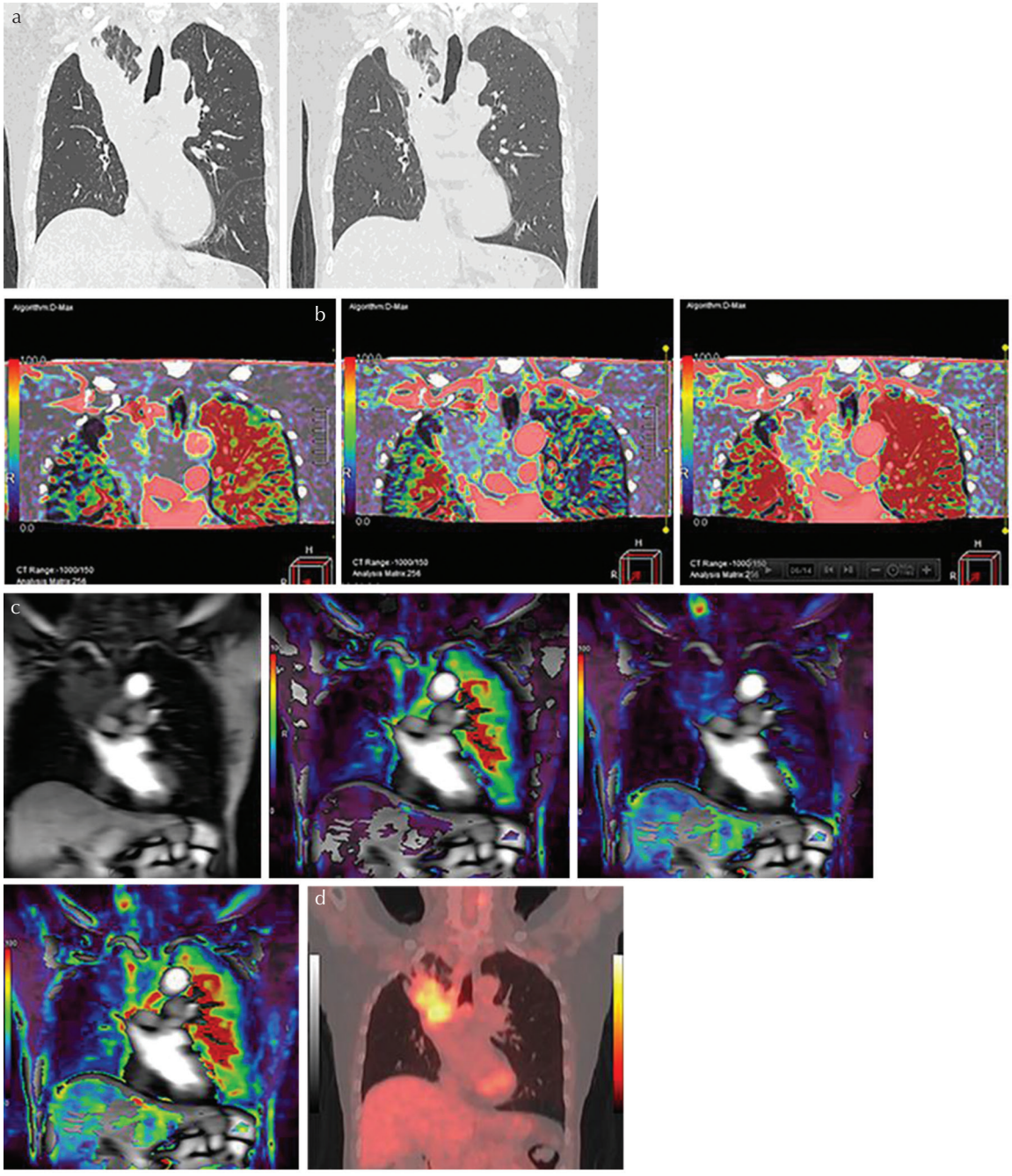

Fig. 1 A 81-year-old male patient with squamous cell carcinoma treated with chemoradiotherapy and assessed as NC. Progression-free and overall survival at 15 and 24 months. (**a**) Thin-section MPR image from thin-section CT data (L to R: MPR images obtained pre- and post-treatment at lung window setting) show lung cancer in the right upper lobe. This case was assessed as NC by response evaluation criteria in solid tumors (RECIST ver.1.1). (**b**) Perfusion maps derived from dynamic first-pass CE-perfusion area detector CT assessed with the dual-input maximum slope method (L to R: pulmonary arterial perfusion, systemic arterial perfusion and total perfusion maps) for the same targeted lesion. Pulmonary arterial perfusion, systemic arterial perfusion and total perfusion were 13.6, 18.9, and 32.5 ml/100 ml/min, respectively. This case was assessed as a RECIST-based non-responder for systemic arterial and total perfusions, and as true-positive. (**c**) Source image and perfusion maps on dynamic first-pass CE-perfusion MR imaging assessed with the dual-input maximum slope method (L to R: source image, pulmonary arterial perfusion, systemic arterial perfusion, and total perfusion maps) for the same targeted lesion. Pulmonary arterial perfusion, systemic arterial perfusion, and total perfusion were 9.2, 28.9, and 38.1 ml/100 ml/min, respectively. This case was also assessed as a RECIST-based non-responder for systemic arterial and total perfusions, and as true-positive. However, this case was evaluated as responder and as false-positive on the basis of pulmonary arterial perfusion findings. (**d**) PET/CT demonstrates high uptake of 2-[fluorine-18]-fluoro-2-deoxy-D-glucose, and SUV_{max} was evaluated as 4.7. This case was evaluated as a RECIST-responder and assessed as false-negative. PR, partial response; MPR, multiplanar reformatted; RECIST, Response Evaluation Criteria in Solid Tumor; CE, contrast-enhanced; SUV, standardized uptake value; PET, positron emission tomography.

Table 1 Comparisons of gender, age, performance status, dynamic first-pass CE-perfusion ADCT and MR indices, SUV_{max}, and length of PFS and OS for RECIST responders and non-responders

	Responders	Non-responders	*P*
Gender			
Male (cases)	14	11	0.76
Female (cases)	9	9	
Age (years old) (Mean ± standard deviation)	66.5 ± 8.6	65.8 ± 9.0	0.06
Performance status (Mean ± standard deviation)	0.1 ± 0.4	0.2 ± 0.7	0.26
Histological subtype			
Adenocarcinoma	20	15	0.31
Squamous cell carcinoma	2	5	
Large cell carcinoma	1	0	
Tumor marker			
Positive	11	14	0.20
Negative	8	20	
Dynamic CE-perfusion ADCT			
Total perfusion (ml/100 ml/min) (Mean ± standard deviation)	38.6 ± 17.6	22.4 ± 6.1	0.0003
Pulmonary arterial perfusion (ml/100 ml/min) (Mean ± standard deviation)	22.5 ± 15.2	14.3 ± 5.2	0.03
Systemic arterial perfusion (ml/100 ml/min) (Mean ± standard deviation)	15.3 ± 8.8	8.1 ± 2.8	0.001
Dynamic CE-perfusion MR imaging			
Total perfusion (ml/100 ml/min) (Mean ± standard deviation)	46.6 ± 18.5	27.2 ± 7.1	<0.0001
Pulmonary arterial perfusion (ml/100 ml/min) (Mean ± standard deviation)	23.6 ± 15.9	15.0 ± 5.5	0.03
Systemic arterial perfusion (ml/100 ml/min) (Mean ± standard deviation)	23.0 ± 13.2	12.2 ± 4.2	0.001
PET/CT			
SUV_{max} (Mean ± standard deviation)	4.7 ± 1.5	6.2 ± 1.5	0.002
PFS (months) (Mean ± standard error)	34.0 ± 4.9	22.9 ± 5.3	0.04
OS (months) (Mean ± standard error)	38.9 ± 5.6	29.4 ± 7.1	0.006

ADCT, area detector computed tomography; CE, contrast-enhanced; OS, overall survival; PFS, progression free survival; PET, positron emission tomography, RECIST, response evaluation criteria in solid tumors; SUV, standardized uptake value.

Utility of radiological indices with significant impact for prediction of therapeutic effect on progression-free and overall survival with Kaplan–Meier method

Results of comparison of PFS and OS of the responder and non-responder groups for each perfusion index-based and SUV_{max}-based biomarkers are shown in Table 3.

Application of each threshold value for differentiating RECIST-based responders and non-responders showed that mean PFS was significantly different for the two groups in terms of total perfusion ($P < 0.05$) and systemic arterial perfusion ($P < 0.05$).

A comparison of mean OS showed significant differences between the responder and non-responder groups in terms of total perfusion ($P < 0.05$) and systemic arterial perfusion ($P < 0.05$). Although there were no significant differences between PFS and OS when the threshold value for distinguishing RECIST-based responders from RECIST-based non-responders was used for SUV_{max}, mean OS of responders assessed as SUV_{max} 8.2 or less was significantly longer than that of non-responders for the same threshold value ($P = 0.02$).

Utility for radiological indices as significant predictors for progression-free and overall survivals with multivariate analyses

As the result of a multivariate analysis with Cox proposal hazard regression model for PFS, significant predictors were determined as systemic arterial perfusions on ADCT (hazard ratio: 19.6, $P = 0.003$) and MR imaging (hazard ratio: 15.9, $P = 0.03$) and SUV_{max} (hazard ratio: 10.3, $P = 0.009$). On the other hand, a multivariate analysis with Cox proposal hazard regression model for OS showed a significant predictor was systemic arterial perfusion on ADCT (hazard ratio: 12.2, $P = 0.04$).

Discussion

Our results demonstrate that dynamic first-pass CE-perfusion ADCT and MR imaging have better potential than FDG-PET/CT to function as early predictors for the therapeutic effect of chemoradiotherapy for NSCLC patients. To the best of our knowledge, this paper was the first paper that demonstrated

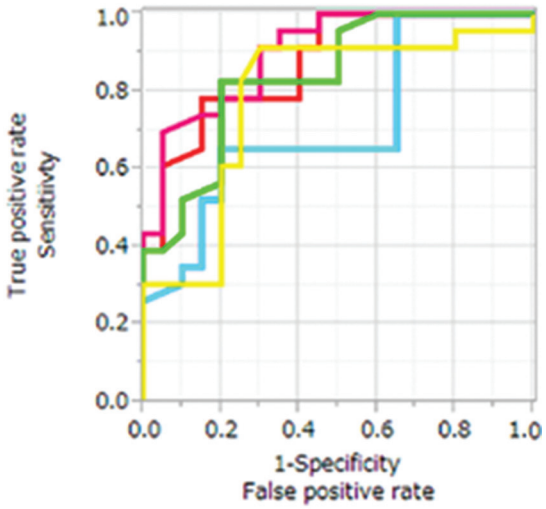

Fig. 2 Receiver operating characteristics analysis of radiological indices disclosed significant differences between the RECIST responder and non-responder groups (red line: total perfusion on dynamic first-pass CE-perfusion ADCT; blue line: pulmonary arterial perfusion on dynamic first-pass CE-perfusion ADCT; green line: systemic arterial perfusion on dynamic first-pass CE-perfusion ADCT; pink line: total perfusion on dynamic first-pass CE-perfusion MR imaging; sky blue line: pulmonary arterial perfusion on dynamic first-pass CE-perfusion MR imaging; yellow-green line: systemic arterial perfusion on dynamic first-pass CE-perfusion MR imaging; yellow: SUV_{max}). AZs for indices on dynamic first-pass CE-perfusion ADCT were as follows: total perfusion, Az = 0.87; pulmonary arterial perfusion, Az = 0.72; systemic arterial perfusion, Az = 0.84. Moreover, Az for indices on dynamic first-pass CE-perfusion MR imaging were as follows: total perfusion, Az = 0.90; pulmonary arterial perfusion, Az = 0.72; systemic arterial perfusion, Az = 0.84. In addition, Az of SUV_{max} was assessed as 0.78. Az for total perfusion on dynamic first-pass CE-perfusion ADCT was significantly larger than that for pulmonary arterial perfusion using either method (ADCT: $P = 0.003$, MR imaging: $P = 0.003$). In addition, Az for total perfusion on dynamic first-pass CE-perfusion MR imaging was significantly larger than that for pulmonary arterial perfusion using either method (ADCT: $P = 0.002$, MR imaging: $P = 0.002$). The feasible threshold values for all indices were determined for dynamic CE-perfusion ADCT (total perfusion, 29.2 ml/100 ml/min; pulmonary arterial perfusion, 15.5 ml/100 ml/min; systemic arterial perfusion, 11.0 ml/100 ml/min), dynamic CE-perfusion MR imaging (total perfusion, 37.5 ml/100 ml/min; pulmonary arterial perfusion, 16.3 ml/100 ml/min; systemic arterial perfusion, 16.5 ml/100 ml/min) and PET/CT (5.7 for SUV_{max}). ADCT, area-detector computed tomography; CE, contrast-enhanced; SUV, standardized uptake value; Az, area under the curve; PET/CT, positron emission tomography combined with CT.

the two dynamic first-pass CE-perfusion methods are similarly effective in this setting.

The comparison of intra-observer agreements for each index assessment showed that all index measurements featured excellent correlation between first and second measurements, and the reproducibility coefficient was satisfactory for clinical purposes as established in previously published studies.[3,9,14–23,26,27]

The comparison of inter-method agreements between dynamic first-pass CE-perfusion ADCT and MR imaging for each index indicated there were significant and excellent correlations between the two methods for all indices and that the limits of agreement for each perfusion index was smaller than the reproducibility coefficient and small enough for clinical purposes.[3,9,14–23,26,27] When the same mathematical model is used, dynamic first-pass CE-perfusion ADCT and MR imaging can be considered to have the same potential for evaluation of the perfusion parameters for therapeutic effect prediction for NSCLC patients. However, linear regression between signal intensity and gadolinium concentration is considered as limited range. Although small amount of gadolinium contrast media was applied in this study, dynamic first-pass CE-perfusion MR indices might have included relative errors.

Comparisons between clinical and patient parameters and radiological indices from dynamic CE-perfusion ADCT and MR imaging as well as PET/CT for responders and non-responders assessed by means of RECIST ver.1.1 criteria demonstrated that all radiological indices, PFS and OS showed significant differences between the responder and non-responder groups. With considering the underlying basic concepts of chemoradiotherapy interactions and the results of pharmacokinetic analyses,[3,14–18,28–30] our results are compatible with the previously published findings for dynamic first-pass CE-perfusion CT and MR imaging in this setting.

The utility of total perfusion and systemic arterial perfusion for differentiating RECIST-based responders from non-responders was significantly superior to that of pulmonary arterial perfusion as observed on dynamic first-pass CE-perfusion ADCT and MR imaging. In addition, there were no significant differences in sensitivity, specificity and accuracy among FDG-PET/CT, dynamic first-pass CE-perfusion ADCT and MR imaging for distinguishing RECIST-based responders from non-responders. This finding was to be expected because, as previously reported, lung cancer receives a dual blood supply, one from the pulmonary artery or capillary bed, and the other from the bronchial artery.[3,14–18,30] Although details of chemoradiation therapy is not entirely known, toxicity, oxygen-derived free radical, interstitial edema, sclerosis of small vessels, especially induced by angiogenesis from bronchial artery and obliteration of a major portion of the capillary bed have been suggested to be influence to therapeutic effect as well as radiation-induced interstitial lung disease such as radiation pneumonitis and fibrosis.[31] Our results are therefore compatible with the underlying biological characteristics of lung cancer patients, and can be considered more reliable as compared with those previously reported.[3,14,15]

Application of each feasible threshold value for distinguishing RECIST-based responders from non-responders to the impact on therapeutic effect prediction of total and systemic arterial perfusions on dynamic first-pass CE-ADCT and MR

Table 2 Capability of radiological indices with a significant difference between RECIST responders and RECIST non-responders for differentiation between the two groups

		Threshold value	SE (%)	SP (%)	PPV (%)	NPV (%)	AC (%)
Dynamic CE-perfusion ADCT	Total perfusion	≤29.2	78.3 (18/23)	85 (17/20)	85.7 (18/21)	77.3 (17/22)	81.4 (35/43)
	Pulmonary arterial perfusion	≤15.5	65.2 (15/23)	80 (16/20)	78.9 (15/19)	66.7 (16/24)	72.1 (31/43)
	Systemic arterial flow	≤11.0	82.6 (19/23)	80 (16/20)	82.6 (19/23)	80 (16/20)	81.4 (35/43)
Dynamic CE-perfusion MR imaging	Total perfusion	≤37.5	69.6 (16/23)	95 (19/20)	94.1 (16/17)	73.1 (19/26)	81.4 (35/43)
	Pulmonary arterial perfusion	≤16.3	65.2 (15/23)	80 (16/20)	78.9 (15/19)	66.7 (16/24)	72.1 (31/43)
	Systemic arterial perfusion	≤16.5	82.6 (19/23)	80 (16/20)	82.6 (19/23)	80 (16/20)	81.4 (35/43)
FDG-PET/CT	SUV_{max}	≤5.7	87 (20/23)	70 (14/20)	76.9 (20/26)	82.4 (14/17)	79.1 (34/43)

ADCT, area detector computed tomography; AC, accuracy; CE, contrast-enhanced; NPV, negative predictive value; PPV, positive predictive value; PET, positron emission tomography, RECIST, response evaluation criteria in solid tumors; SUV, standardized uptake value; SE, sensitivity; SP, specificity.

Table 3 Comparison of progression-free and overall survival for responder and non-responder groups determined with indices with a significant influence therapeutic effect

Methods	Indices	Threshold value		Progression-free survival (months)		Overall survival (months)	
				(Mean ± SE)	*P*	(Mean ± SE)	*P*
Dynamic first-pass CE-perfusion ADCT	Total perfusion (ml/100 ml/min)	≤29.2	Responders	34.4 ± 4.5	0.04	47.8 ± 7.6	0.009
			Non-responders	14.1 ± 1.2		24.3 ± 3.5	
	Pulmonary arterial perfusion (ml/100 ml/min)	≤15.5	Responders	34.1 ± 4.5	0.07	35.8 ± 5.6	0.09
			Non-responders	14.3 ± 1.2		15.6 ± 2.4	
	Systemic arterial perfusion (ml/100 ml/min)	≤11.0	Responders	40.6 ± 4.3	0.003	60 ± 12	0.0006
			Non-responders	18.9 ± 3.3		25.6 ± 3.7	
Dynamic first-pass CE-perfusion MR imaging	Total perfusion (ml/100 ml/min)	≤37.5	Responders	38.4 ± 4.8	0.004	52.8 ± 8.1	0.003
			Non-responders	13.7 ± 1.1		25.2 ± 2.8	
	Pulmonary arterial perfusion (ml/100 ml/min)	≤16.3	Responders	28.1 ± 3.9	0.52	38.2 ± 5.8	0.68
			Non-responders	5.8 ± 0.3		12 ± 1	
	Systemic arterial perfusion (ml/100 ml/min)	≤16.5	Responders	33.4 ± 4.2	0.02	46.4 ± 6.9	0.001
			Non-responders	12.7 ± 1.1		19.1 ± 1.7	
PET/CT	SUV_{max}	≤5.7	Responders	30.3 ± 4.7	0.81	39.8 ± 8.3	0.98
			Non-responders	29.2 ± 6		38.2 ± 8.6	
		≤8.2	Responders	29.8 ± 3.7	0.47	40 ± 5.8	0.02
			Non-responders	12 ± 0.3		15 ± 0.2	

ADCT, area-detector computed tomography; CE, contrast-enhanced; SUV, standardized uptake value; PET/CT, positron emission tomography combined with CT; SE, Standard error.

imaging, showed significant differences in PFS and OS. However, when similar threshold values were applied to SUV_{max}, there were no such significant differences. On the other hand, when different threshold value was used for SUV_{max}, only OS was significantly different for the two groups. In addition, a multivariate analysis with Cox proposal hazard regression model showed systemic arterial perfusions on ADCT and MR imaging as well as SUV_{max} as significant predictors for PFS, and systemic arterial perfusion on ADCT as significant predictor for OS in NSCLC patients with chemoradiotherapy. Therefore, dynamic first-pass CE-perfusion ADCT and MR imaging can be considered to be as equal to or more useful than PET/CT in this setting. In addition, perfusion matrixes, especially systemic arterial perfusion, are

suggested as having equal to or better potential for therapeutic effect prediction than glucose metabolism in NSCLC patients treated with chemoradiotherapy.

Our study has a limitation. Although we used our proprietary software for this study, and the mathematical models used in this software were basic and are fully detailed in this paper and others,[3,14–23] only a few vendors provide software for assessment of perfusion for dynamic CE-perfusion CT and dynamic CE-MR imaging. Therefore, further comparisons with other software as well as radiological methods for assessing tumor perfusion are warranted to validate the clinical relevance of tumor perfusion assessment results obtained in this setting.

Conclusion

Dynamic first-pass CE-perfusion ADCT and MR imaging are as useful as PET/CT for early prediction of treatment response of NSCLC patients treated with chemoradiotherapy. In addition, when the same mathematical model is used for both dynamic first-pass CE-perfusion methods, tumor perfusion assessments for such patients can also be performed by dynamic first-pass CE-perfusion ADCT and MR imaging.

Acknowledgments

The authors wish to thank Toshinori Sekitani, RT, Wakiko Tani, RT, Noriyuki Negi, RT, Katsusuke Kyotani, RT, Satoru Takahashi, MD, PhD (all from the Center for Radiology and Radiation Oncology, Kobe University Hospital), Shintaro Tokunaga, MD, Shuya Hori, MD, PhD, Motoko Tachihara, MD, Daisuke Tamura, MD, PhD, Kazuyuki Kobayashi, MD, PhD, Yoshihiro Nishimura, MD, PhD (all from the Division of Respiratory Medicine, Department of Internal Medicine, Kobe University Graduate School of Medicine), Yasuo Ejima, MD, PhD, Ryohei Sasaki, MD, PhD (all from the Division of Radiation Oncology, Department of Radiology, Kobe University Graduate School of Medicine), and Hideki Nishimura, MD, PhD (Department of Radiation Oncology, Kobe Minimally Invasive Cancer Center) for their valuable contributions to this study.

Funding

This work was supported by Grants-in-Aid for Scientific Research from the Japanese Ministry of Education, Culture, Sports, Science and Technology (JSTS.KAKEN; No. 24591762), the Adaptive and Seamless Technology Transfer Program through Target Driven R & D from the Japan Science and Technology (JST) Agency (AS2511335P), Canon Medical Systems Corporation, Bayer Pharma and Guerbet Japan.

Conflicts of Interest

Drs. Ohno, Yoshikawa and Seki had research grants from Grants-in-Aid for Scientific Research from the Japanese Ministry of Education, Culture, Sports, Science and Technology (JSTS.KAKEN; No. 24591762), Canon Medical Systems Corporation, Bayer Pharma and Guerbet Japan. Dr. Ohno and Ms. Fujisawa had research grant from the Adaptive and Seamless Technology Transfer Program through Target Driven R & D from the Japan Science and Technology (JST) Agency (AS2511335P).

Four of the authors (Yasuko Fujisawa, Masao Yui, Shigeharu Ohyu and Naoki Sugihara), who are employees of Canon Medical Systems Corporation, developed the software, but had no control over any data or information submitted for publication or any control over any parts of data and information included in this study.

References

1. Aupérin A, Le Péchoux C, Rolland E, et al. Meta-analysis of concomitant versus sequential radiochemotherapy in locally advanced non-small-cell lung cancer. J Clin Oncol 2010; 28:2181–2190.
2. Mac Manus MP, Hicks RJ, Matthews JP, et al. Positron emission tomography is superior to computed tomography scanning for response-assessment after radical radiotherapy or chemoradiotherapy in patients with non-small-cell lung cancer. J Clin Oncol 2003; 21:1285–1292.
3. Ohno Y, Nogami M, Higashino T, et al. Prognostic value of dynamic MR imaging for non-small-cell lung cancer patients after chemoradiotherapy. J Magn Reson Imaging. 2005; 21:775–783.
4. Mac Manus M, Hicks RJ, Everitt S. Role of PET-CT in the optimization of thoracic radiotherapy. J Thorac Oncol. 2006; 1:81–84.
5. Wang J, Wu N, Cham MD, Song Y. Tumor response in patients with advanced non-small cell lung cancer: perfusion CT evaluation of chemotherapy and radiation therapy. AJR Am J Roentgenol 2009; 193:1090–1096.
6. Ng QS, Goh V, Milner J, et al. Quantitative helical dynamic contrast enhanced computed tomography assessment of the spatial variation in whole tumour blood volume with radiotherapy in lung cancer. Lung Cancer 2010; 69:71–76.
7. Fraioli F, Anzidei M, Zaccagna F, et al. Whole-tumor perfusion CT in patients with advanced lung adenocarcinoma treated with conventional and antiangiogenetic chemotherapy: initial experience. Radiology 2011; 259:574–582.
8. Yabuuchi H, Hatakenaka M, Takayama K, et al. Non-small cell lung cancer: detection of early response to chemotherapy by using contrast-enhanced dynamic and diffusion-weighted MR imaging. Radiology 2011; 261:598–604.
9. Ohno Y, Koyama H, Yoshikawa T, et al. Diffusion-weighted MRI versus ^{18}F-FDG PET/CT: performance as predictors of tumor treatment response and patient survival in patients with non-small cell lung cancer receiving chemoradiotherapy. AJR Am J Roentgenol 2012; 198: 75–82.
10. Tacelli N, Santangelo T, Scherpereel A, et al. Perfusion CT allows prediction of therapy response in non-small cell lung cancer treated with conventional and anti-angiogenic chemotherapy. Eur Radiol 2013; 23:2127–2136.

11. Hwang SH, Yoo MR, Park CH, Jeon TJ, Kim SJ, Kim TH. Dynamic contrast-enhanced CT to assess metabolic response in patients with advanced non-small cell lung cancer and stable disease after chemotherapy or chemoradiotherapy. Eur Radiol 2013; 23:1573–1581.
12. Nishino M, Hatabu H, Johnson BE, McLoud TC. State of the art: response assessment in lung cancer in the era of genomic medicine. Radiology 2014; 271:6–27.
13. Sudarski S, Shi J, Schmid-Bindert G, et al. Dynamic volume perfusion computed tomography parameters versus RECIST for the prediction of outcome in lung cancer patients treated with conventional chemotherapy. J Thorac Oncol 2015; 10:164–171.
14. Ohno Y, Koyama H, Fujisawa Y, et al. Dynamic contrast-enhanced perfusion area detector CT for non-small cell lung cancer patients: influence of mathematical models on early prediction capabilities for treatment response and recurrence after chemoradiotherapy. Eur J Radiol 2016; 85:176–186.
15. Ohno Y, Fujisawa Y, Koyama H, et al. Dynamic contrast-enhanced perfusion area-detector CT assessed with various mathematical models: its capability for therapeutic outcome prediction for non-small cell lung cancer patients with chemoradiotherapy as compared with that of FDG-PET/CT. Eur J Radiol 2017; 86:83–91.
16. Ohno Y, Koyama H, Matsumoto K, et al. Differentiation of malignant and benign pulmonary nodules with quantitative first-pass 320-detector row perfusion CT versus FDG PET/CT. Radiology 2011; 258:599–609.
17. Ohno Y, Nishio M, Koyama H, et al. Comparison of quantitatively analyzed dynamic area-detector CT using various mathematic methods with FDG PET/CT in management of solitary pulmonary nodules. AJR Am J Roentgenol 2013; 200:W593–W602.
18. Ohno Y, Nishio M, Koyama H, et al. Solitary pulmonary nodules: comparison of dynamic first-pass contrast-enhanced perfusion area-detector CT, dynamic first-pass contrast-enhanced MR imaging, and FDG PET/CT. Radiology 2015; 274:563–575.
19. Ohno Y, Hatabu H, Murase K, et al. Quantitative assessment of regional pulmonary perfusion in the entire lung using three-dimensional ultrafast dynamic contrast-enhanced magnetic resonance imaging: preliminary experience in 40 subjects. J Magn Reson Imaging 2004; 20:353–365.
20. Ohno Y, Hatabu H, Murase K, et al. Primary pulmonary hypertension: 3D dynamic perfusion MRI for quantitative analysis of regional pulmonary perfusion. AJR Am J Roentgenol 2007; 188:48–56.
21. Ohno Y, Koyama H, Nogami M, et al. Dynamic perfusion MRI: capability for evaluation of disease severity and progression of pulmonary arterial hypertension in patients with connective tissue disease. J Magn Reson Imaging 2008; 28:887–899.
22. Ohno Y, Koyama H, Matsumoto K, et al. Dynamic MR perfusion imaging: capability for quantitative assessment of disease extent and prediction of outcome for patients with acute pulmonary thromboembolism. J Magn Reson Imaging 2010; 31:1081–1090.
23. Ohno Y, Koyama H, Yoshikawa T, et al. Contrast-enhanced multidetector-row computed tomography vs. time-resolved magnetic resonance angiography vs. contrast-enhanced perfusion MRI: assessment of treatment response by patients with inoperable chronic thromboembolic pulmonary hypertension. J Magn Reson Imaging 2012; 36:612–623.
24. Schoenfeld C, Cebotari S, Hinrichs J, et al. MR imaging-derived regional pulmonary parenchymal perfusion and cardiac function for monitoring patients with chronic thromboembolic pulmonary hypertension before and after pulmonary endarterectomy. Radiology 2016; 279: 925–934.
25. Eisenhauer EA, Therasse P, Bogaerts J, et al. New response evaluation criteria in solid tumours: revised RECIST guideline (version 1.1). Eur J Cancer 2009; 45:228–247.
26. Bland JM, Altman DG. Statistical methods for assessing agreement between two methods of clinical measurement. Lancet 1986; 1:307–310.
27. Bland JM, Altman DG. Comparing methods of measurement: why plotting difference against standard method is misleading. Lancet 1995; 346:1085–1087.
28. Philips TL. Radiation-chemotherapy interaction, In: Pass HI, Mitchell JB, Johnson DH, Turrisi AT, eds. Lung Cancer Principles and Practice. Philadelphia: Lippincott-Raven, 1996; 251–270.
29. Robins. Environmental and nutritional pathology, In: Cotran RS, Kumar V, Collins T, eds. Pathologic Basis of Disease, 6th ed. Philadelphia: W.B. Saunders, 1999; 403–491.
30. Ohno Y, Nishio M, Koyama H, et al. Dynamic contrast-enhanced CT and MRI for pulmonary nodule assessment. AJR Am J Roentgenol 2014; 202:515–529.
31. Weinberger SE. Interstitial diseases associated with known etiology agent, In: Weinberger SE, ed. Principle of Pulmonary Medicine, 3rd ed. Philadelphia, London, New York, St. Louis, Sydney, Toronto: W.B. Saunders, 1998; 141–153.